Title: Drought phenotyping in Vitis vinifera using RGB and NIR imaging

Corresponding Author: Dr. Giuseppe Montanaro, PhD

Corresponding Author's Institution: Università degli Studi della Basilicata

First Author: Nunzio Briglia, PhD candidate

Order of Authors: Nunzio Briglia, PhD candidate; Giuseppe Montanaro, PhD; Angelo Petrozza, Dr.; Stephan Summerer, Dr.; Francesco Cellini, Dr.; Vitale Nuzzo, Dr.

Abstract: This study examined whether morphophysiological traits (i.e., leaf area, plant water consumption, leaf water potential) of drought stressed grapevines (Vitis vinifera L.) might be determined through the use of non-destructive RGB and NIR image-based analysis techniques for possible implementation of affordable phenotyping. The study was carried out at a centre which is part of the European Plant Phenotyping Network (EPPN) also aiming at contribute to the standardisation of phenotyping protocols.

Four groups of 20 potted vines each were subjected to various irrigation treatments restoring 100% (control), 75% (IRR75%), 50% (IRR50%) and 25% (IRR25%) of their daily water consumption within a 22-day period of drought imposition. Leaf gas exchanges, leaf water potential (Ψ, photosystem II efficiency (Fv/Fm), RGB and NIR data were simultaneously collected during drought imposition. Values of Ψ in IRR25% vines reached -1.2 MPa pre-dawn, in turn stomatal conductance and net photosynthetic rate reached values as low as approx. 0.02 mol H_2O m-2 s-1 and 1.0 µmol CO_2 m-2 s-1, respectively. Through a cross-validation analysis, this study modelled (R^2=0.78) the estimation of plant canopy area based on the number of pixel of RGB images of vines under various drought levels. Estimated leaf area was employed to calculate water consumption per unit leaf area, which resulted correlated (R^2=0.86) with Ψ.

Results revealed a correlation between Ψ and Dark Green colour class (R^2=0.71) and suggest a new working hypothesis concerning the phenotyping of leaf (or petiole) angle. NIR and Dark Green colour fraction decreased with increasing levels of drought while the Yellow one increased. The outcomes presented may strengthen the role of RGB and NIR based images to identify the occurrence of water-stress in Vitis spp. and contribute to

both the standardisation of phenotyping protocols pursued by the global phenotyping community and the possible development of new tools for precision irrigation in a HTP domain.

COVER LETTER

Università degli Studi della Basilicata

Dipartimento delle Culture Europee e del Mediterraneo: Architettura, Ambiente, Patrimoni culturali (DiCEM)

Matera, May 31st 2019

To:
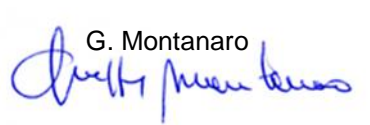
The Editor-in Chief

Scientia Horticulturae

Dear Sir,

We appreciated the favourable position of the Editorial Board concerning the potential acceptance of the manuscript. Now I'm submitting the revised version of the manuscript titled "Drought phenotyping in *Vitis vinifera* using RGB and NIR imaging" Ms. No. **HORTI23411R1** for the re-evaluation for publication in *Scientia Horticulturae*.

The manuscript has been revised accepting the comments received by Reviewer #1, and we thanks the reviewer #3 for his/her positive comments. Minor changes have been written in red in the revised version.

We hope this revised version of the manuscript could be found appropriate for publication in *Scientia Horticulturae*.

We look forward to your next communication. Please let me know if you need any further information. Sincerely yours,

G. Montanaro

(SCOPUS ID: 12778359900)

Manuscript ID HORTI23411R1

TITLE " **Drought phenotyping in *Vitis vinifera* using RGB and NIR imaging**"

Answer to *Reviewer #1 comments.*

1. *I understand that the imaging system provides you with some colour classes, which do not correspond by any means with spectral bands. I do not know if this is fully clarified in the manuscript. Please do it in the M&M section.*

Thanks for your comment. In order to further improve the clarity of the text, in a couple of sentences we specify that the RGB images were sourced by Visible light camera (please refer to lines 139 of the M&M section), in turn also the Line 380 was slightly reworded.

2. *Do you know if the embedded process for colour classification is based on Mahalanobis algorithm or similar? Did you choose the pixel seeds to define the different color classes or were they pre-configured in the system? Please include some info.*

Thanks for your comments, unfortunately the user manual of the LemnaTec Grid software does not report any clear information on the algorithm(s) adopted for the colour class classification. At the paragraph "*8.2.2.5.1.1.3.1 Device- Colour classification*" it is reported that the colour of each single pixel is assigned with a procedure based on the "*Euklidan distance in RGB space*". We believe that this general information might be of very limited interest for readers because no clear algorithm description is provided, hence we do not add it in the revised version. The vagueness of the algorithm used might likely be in some way due to a confidential nature of that information.
By a scientific point of view, the replicability of the study is allowed because all information on LemnaTec machines and software employed were provided, ultimately considering that the LemnaTec software is not an open source, the deep knowledge of the algorithm used for colour class classification would not be useful for potential customization.

Concerning the choice of the pixel seeds (corresponding to the "anchor points" in the LemnaTecGrid software manual), it was operated but we were not accurate in reporting it in the M&M section. At the beginning of the image analysis, two anchor points (RGB colour values) per each colour class were identified as follow: Dark Green R126 G134 B68, R116 G123 B75; Green R156 G170 B87, R150 G177 B73; Yellow R255 G242 B157, R255 G244 B116; Brown R133 G104 B67, R124 G107 B60. This information is now included in the revised ms (please refer to 149-151 lines)

3. *Regarding the combination of PD and MD stem water potential. The papers you include as examples do not combine measurements of a given physiological variable at different times of the day with the same purpose as you do in your work (you want to run a regression, they don't). For this reason I still think this combination is completely sound, but I will not go further on this.*
Thank you.

Line 437. Please remove "reflectance" after RGB
DONE, please refer to line 447 of the revised ms

Line 834 (Figure 10 caption). Add "classes" after Dark Green

DONE

Drought phenotyping in *Vitis vinifera* using RGB and NIR imaging

By N. Briglia et al.

- This study examined whether morphophysiological traits (e.g., leaf water potential, Ψ) of drought stressed grapevines might be determined through image-based analysis techniques
- Non-destructive image-based method for the prediction of leaf area in drought stressed vines ($R^2 = 0.92$) is presented
- The Dark Green fraction colour class correlates ($R^2 = 0.71$) with Ψ.
- Data presented support the development of affordable phenotyping and standardization of protocols

Drought phenotyping in *Vitis vinifera* using RGB and NIR imaging

Nunzio Briglia[1], Giuseppe Montanaro[1*], Angelo Petrozza[2], Stephan Summerer[2], Francesco Cellini[2], Vitale Nuzzo[1]

[1]Dipartimento delle Culture Europee e del Mediterraneo - Università degli Studi della Basilicata – (Italy)

[2]ALSIA Centro Ricerche Metapontum Agrobios, s.s. Jonica 106, km 448,2, Metaponto, MT 75010, Italy

*Corresponding author

E-mail: giuseppe.montanaro@unibas.it   Phone ++39 391 3808337

ORCiD http://orcid.org/0000-0002-1172-7526

Address:

Università degli Studi della Basilicata - Dipartimento delle Culture Europee e del Mediterraneo, Via S. Rocco, 3 – 75100 Matera (Italy)

1   **Abstract** This study examined whether morphophysiological traits (i.e., leaf area, plant water

2   consumption, leaf water potential) of drought stressed grapevines (*Vitis vinifera* L.) might be

3   determined through the use of non-destructive RGB and NIR image-based analysis techniques for

4   possible implementation of affordable phenotyping. The study was carried out at a centre which is

5   part of the *European Plant Phenotyping Network* (EPPN) also aiming at contribute to the

6   standardisation of phenotyping protocols. Four groups of 20 potted vines each were subjected to

7   various irrigation treatments restoring 100% (control), 75% ($IRR_{75\%}$), 50% ($IRR_{50\%}$) and 25%

8   ($IRR_{25\%}$) of their daily water consumption within a 22-day period of drought imposition. Leaf gas

9   exchanges, leaf water potential (Ψ), photosystem II efficiency (F_v/F_m), RGB and NIR data were

10   simultaneously collected during drought imposition. Values of Ψ in $IRR_{25\%}$ vines reached -1.2 MPa

11   pre-dawn, in turn stomatal conductance and net photosynthetic rate reached values as low as

12   approx. 0.02 mol H_2O m^{-2} s^{-1} and 1.0 µmol CO_2 m^{-2} s^{-1}, respectively. Through a cross-validation

13   analysis, this study modelled (R^2=0.78) the estimation of plant canopy area based on the number of

14   pixel of RGB images of vines under various drought levels. Estimated leaf area was employed to

15   calculate water consumption per unit leaf area, which resulted correlated (R^2=0.86) with Ψ. Results

16   revealed a correlation between Ψ and Dark Green colour class (R^2=0.71) and suggest a new

17   working hypothesis concerning the phenotyping of leaf (or petiole) angle. NIR and Dark Green

18   colour fraction decreased with increasing levels of drought while the Yellow one increased. The

19   outcomes presented may strengthen the role of RGB and NIR based images to identify the

20   occurrence of water-stress in *Vitis* spp. and contribute to both the standardisation of phenotyping

21   protocols pursued by the global phenotyping community and the possible development of

22   new tools for precision irrigation in a HTP domain.

23

24   **Key words:** affordable phenotyping, EPPN, grapevine, image analysis, leaf gas exchanges,

25   water potential, water stress.

26

1. Introduction

27

28   Drought occurrence is expected to increase in some cultivated areas due to future

29   uncertainty in precipitations resulting mainly from climate changes, this in turn will reduce

30   stock of freshwater for irrigated agricultural sector (IPCC, 2013; Ronco et al., 2017)

31   requiring adaptation strategies including improved on-farm irrigation management.

32   Although drought occurrence negatively influence certain plant performances (e.g., fruit

33   size, carbon gain) (Miller et al., 1998; Shackel, 2007), the exposure of plant to drought

34   might favour fruit quality traits depending on timing, intensity, duration of drought and

35   crop species (Chaves, et al., 2010; Herrero-Langreo, et al., 2018). For instance, in grape

36   berries the amount of key quality pigments (e.g., total anthocyanins) measured at harvest is

37   higher in drought stressed vines compared to well irrigated ones (Acevedo-Opazo et al.,

38   2010). Hence, irrigation management might potentially be relevant for both the

39   conservation of natural resources (through water saving) and increased quality of product.

40

41   In addition to real time soil moisture probes, the measurements of several *in vivo* plant

42   physiological parameters have been proposed for irrigation schedule including sap flow,

43   stomatal conductance, leaf turgor pressure, shrinkage of stem/fruit, leaf (or stem) water

44   potential (Ψ) (Fernández, 2017). Some of these crop (i.e., soil and plant) parameters are

45   collectively feeding most of the irrigation decision support systems now increasingly

46   accepted by growers due to their decreasing price; however sensor reliability is still

47   perceived as a weakness (Lichtenberg et al., 2015). Leaf water potential is a reliable plant

48   water status indicator for irrigation scheduling but its application at large scale (e.g.,

49   commercial field) is hampered by the high costs (including time) needed for timely and

50   adequately representative Ψ determinations (Girona et al., 2006, De Bei et al., 2010).

51   Hence, a wider adoption of Ψ as irrigation schedule tool might be boosted by the

52   development of easy accessible, accurate and low-cost proxy of Ψ.

53

54   Precision agriculture is challenging the reduction of environmental impact of practices and

55   the improvement of product quality through a series of smart tools including plant

56   phenotyping as supported by image analysis techniques (Fiorani and Schurr, 2013). In this

57   context, some recently developed high-throughput phenotyping (HTP) innovations

58   including unmanned aerial vehicles (UAV), robotised platforms and colour image-derived

59   indices are promising tools for irrigation managing purpose (Berger et al., 2010; Gago et

60   al., 2017; Diago et al., 2018). However, the infrastructure and man-labour cost as well as

61   skills for operational HTP are debatable highlighting the importance of "affordable

62   phenotyping" (Reynolds et al., 2018).

63

64   Recently, the estimation of the vineyard water status using multispectral imagery from an

65   UAV platform and machine learning algorithm based on artificial neural networks have

66   been proposed (Poblete et al., 2017; Romero et al., 2018; Fernández-Novales et al., 2018)

67   but encompassing relatively complex procedures to the extent that the combination of

68   several (up to 13) vegetation indices were needed. This complexity might slow its large

69   scale diffusion (Rinaldi and He, 2014). According to this view it makes sense to evoke

70   Rapaport and co-workers (2015) who developed water balance indices able to predict Ψ

71   based on reflectance values at specific wavelengths (1 nm spectral resolution). However, it

72   seems there is room to expand affordable phenotyping of Ψ.

73

74   Automated phenotyping of plant stress responses are mainly based on red-green-blue

75   (RGB), fluorescence, near infrared (NIR) (e.g. Casadesus et al., 2007; Harbinson et al.,

76   2012; Diago et al. 2018) and thermal IR imaging systems (e.g. Grant et al., 2007; Cohen et

77   al., 2015; Bellvert et al., 2016; Gutiérrez et al., 2018), with RGB the most frequently used

78   imaging module (Ge et al., 2016). In addition, RGB images have been used also at field

79   scale to model canopy structure, plant growth, irrigation schedule, etc. thanks to their

80   relatively low-cost and wide accessibility as seen by the use of even smartphone cameras

81   (see Reynolds et al., 2018 for review). However specific information on RGB-based images

82   and Ψ correlation in *Vitis* spp. are not adequately explored. Therefore, this study examined

83   whether Ψ of grapevines subjected to drought would be correlated to RGB and NIR

84   images.

85   Nowadays phenotyping biotic and abiotic stress is growing fast and standardisation of

86   phenotyping protocols is becoming a common challenge (van Eeuwijk et al., 2018) where

87   making parallel measurements of physiological and phenomic traits are highly desirable

88   particularly under drought stress. Hence, in this study physiological traits (e.g., leaf gas

89   exchanges, efficiency of photosystem II, plant water consumption) were simultaneously

90   monitored along with Ψ and RGB and NIR images acquisition.

91

92 Leaf area (*LA*) represents almost the entire plant transpiring surface directly influencing

93 plant water consumption and therefore it is a classical key parameter for irrigation

94 management embedded as crop coefficient within crop water balance calculations

95 (Doorenbos and Pruitt, 1977). Hence, a non-destructive estimation of *LA* might assist in

96 defining HTP-based protocols for drought management. For this reason this study also

97 aimed at improving *LA* estimation through RGB-based images and to test whether water

98 consumption per unit of estimated *LA* correlates with Ψ of progressively drought stressed

99 vines.

100

101

2. Materials and methods

103 *2.1 Plant material and experimental design*

104 The experiment was carried out at the ALSIA 'Metapontum Agrobios' Research Centre,

105 located at Metaponto, Southern Italy (N 40° 23' E 16° 47') during the 2017 growing season

106 under unheated and not-conditioned greenhouse conditions. A total of 80 3-year old own-

107 rooted vines (cv Aleatico) were grown in a white 3.5 L PVC pot covered with plastic film

108 to minimise direct evaporation of water from soil. The substrate was a 3:1 v/v mixture of

109 sandy loam soil (82 % sand, 7 % silt and 11 % clay) and peat. At 15, 30 and 45 days after

110 bud-break (early March) the vines were fertilised with a NPK fertiliser 14.7.14 (Slowenne

111 212, Valagro Spa, Atessa, Italy) at a dose of 3 g per pot. From bud-break till the first day of

112 irrigation treatment application (21st of April, hereafter referred as "day 0") all vines were

113 fully irrigated. Vines were weighed every evening and 100% of the amount of water

114   transpired daily was added to keep soil moisture at field capacity. The vines were trained

115   with single main shoot and tied to a wooden stick supports, note that the wooden stick was

116   painted blue in order facilitate image segmentation and data analysis. The vines had approx.

117   15-20 leaves each.

118   Before the imposition of drought stress the reference weight at the field capacity was

119   determined by fully irrigating each pot and then allowing the water to drain for 12 hours

120   until a stable weight was reached.

121   At day 0, vines were grouped ($\times$20 vines each) and for the 22 days after drought imposition

122   (DADI), irrigation (*IRR*) was modulated by restoring 100% (control), 75% (*IRR*$_{75\%}$), 50%

123   (*IRR*$_{50\%}$) and 25% (*IRR*$_{25\%}$) of the daily water consumption.

124   Air temperature (°C) and relative humidity (%RH) (HUMITER 50Y, Vaisala, Helsinki,

125   Finland) and PAR (PPFD, μmol m^{-2} s^{-1}) (quantum sensor Model SKP 215, Skye

126   Instruments LTD, Llandrindod, Wells, UK) were measured inside the greenhouse at 15 min

127   intervals, having hourly averages recorded (CR200, Campbell Scientific Inc., Utah, USA).

128   The air vapour pressure deficit (*VPD*) was then calculated from the records of air

129   temperature and relative humidity, according to Goudriaan and van Laar (1994).

130

131   *2.2 Plant-phenotyping*

132   A group of 4-5 vines per irrigation treatment (the same used for the physiological

133   determinations, see below) were imaged pre-dawn (04:00-05:00 h solar time) and midday

134   (12:00-13:00 h) at 0, 3, 6, 11, 14, 19 and 22 DADI using a LemnaTec 3D Scanalyzer

135   phenotyping platform (LemnaTec GmbH, Aachen, Germany). Vines were automatically

conveyed into the imaging chambers in which they were stopped for image acquisition. The NIR chamber was equipped with a NIR cameras sensitive to wavelength 900-1700 nm (Vosskühler GmbH NIR-300PGE) with the 790 kilopixel resolution. The Visible light chamber for the RGB image acquisition was equipped with 2 megapixel Visible light cameras (Basler Scout scA1600-14gc). Lighting conditions inside the chambers were achieved by halogen lamps (Radium Ralogen PAR16 35W) for the NIR chamber and fluorescent tubes (Osram T5FH 21W 865 HE) for the Visible light chamber. A schematic representation of the plant phenotyping platform set up is reported in Figure 1. For each chamber 3 images were acquired, one from above the plant (Top View, TV) and 2 from the lateral at an orthogonal angle (0° and 90° Side View, SV). The image segmentation and analysis were performed using the software LemnaGrid v5 following Arvidsson et al. (2011). The LemnaGrid software v5 operated a colour classification of the RGB images in Dark Green, Green, Yellow and Brown colour class according to Acosta-Gamboa et al. (2017). Two anchor points (RGB colour values) per colour class were identified as follow: Dark Green R126 G134 B68, R116 G123 B75; Green R156 G170 B87, R150 G177 B73; Yellow R255 G242 B157, R255 G244 B116; Brown R133 G104 B67, R124 G107 B60.

2.3 Leaf gas exchange and chlorophyll a (Chl-a) fluorescence

<u>Net photosynthetic rate</u> (A), stomatal conductance (g_s) and transpiration (E) rate per unit leaf area were measured midday (11:30-12:30 h) at day 0, 3, 6, 8, 10, 11, 13, 14, 20 and 22 DADI using a portable photosynthesis system Li-Cor 6400 (Li-Cor, Inc., Lincoln, NE, USA). During leaf gas exchange measurements temperature and CO_2 concentration were

159 maintained at the prevailing environmental condition, PAR inside the cuvette fixed at 800

160 μmol m^{-2} s^{-1} and the operating flow rate at 500 μmol s^{-1}.

161 Gas exchange measurements were performed on 4-5 vines per irrigation treatment on two

162 fully expanded leaves per vine selected from the mid-region (fourth/fifth node) of shoot.

163

164 On the same leaf used for leaf gas exchange measurements, Chl-*a* fluorescence was

165 measured pre-dawn (04:00 – 05:00 h) and midday (11:30-12:30 h) through a portable

166 chlorophyll fluorometer (PAM- 2500, Heinz Walz GmbH, Effeltrich, Germany). Leaves

167 were 45 min dark-adapted (leaf clip DLC-8 Walz GmbH, Effeltrich, Germany) before

168 midday measurements.

169 The basal (F_0) and maximal (F_m) Chl-*a* fluorescence were collected by applying a brief

170 saturating light pulse (5,000 μmol m^{-2} s^{-1} PAR) and used to calculate the variable

171 fluorescence ($F_v=F_m-F_0$). The maximum quantum yield of photosystem (PS) II (F_v/F_m) was

172 then calculated (Maxwell and Johnson, 2000).

173

174 *2.4 Stem water potential and soil moisture*

175 At 0, 3, 11, 14 and 22 DADI the stem water potential (Ψ) was measured pre-dawn (Ψ_{PD})

176 (04:00 – 05:00 h) and at midday (Ψ_{MD}) (12:00 – 13:00 h) on fully expanded leaves (2 per

177 vine) immediately above those used for gas exchanges by means of a pressure chamber

178 (Model 600, PMS Instruments, Corvallis, OR), pressurised with N$_2$ according to the

179 protocol by Turner (1981). For the Ψ_{MD} determination leaves were covered with aluminium

180 foil at least 90 min before measurements were taken. The leaves used for the Ψ

181   determinations were then collected for leaf area measurement (see below). After the Ψ_{MD}

182   measurements, from the same pots soil samples were collected for soil moisture

183   determination (% of dry weight) according to Black (1965).

184

185

186   *2.5 Estimation and evolution of leaf area*

187   Leaf area of vines was modelled using the RGB images collected for plant phenotyping

188   (see above) determining the number of "plant object pixels" here referred as the projected

189   shoot area (PSA) following a procedure similar to that of Hairmansis et al. (2014):

190

191    $\text{PSA} = N_{pix}\,0°\,\text{SV} + N_{pix}\,90°\,\text{SV} + 0.3 \times N_{pix}\,\text{TV}$ (pixel)   [1]

192

193   where "$N_{pix}\,0°\,\text{SV}$" and "$N_{pix}\,90°\,\text{SV}$" is the number of pixels corresponding to the plant

194   object area of two orthogonal side-view images, while TV represents the number of pixel of

195   the top view image. The pixel numbers were retrieved from the RGB images employing an

196   image analysis pipeline developed using the LemnaGrid v5 software (Petrozza et al., 2014).

197

198   The RGB images for the PSA determination were collected midday on a total of 61 vines

199   randomly selected within each irrigation treatment at day 3, 11, 14 and 22 after the

200   initiation of drought stress. After the image collection vines were manually defoliated and

201   leaf area measured (*LA*) (LI-3100 leaf area meter, LI-COR, Lincoln, NE, USA). Note that

202   pixel number and area of leaves used for Ψ determination were also included for PSA and

203   *LA* determinations.

204

205   The estimated plant leaf area (*LA'*) was modelled using a linear model (*LA'* = a $\times$ *PSA*+b)

206   developed from the paired PSA and *LA* data subjected to a cross-validation analysis. That is,

207   from the whole set of 45 paired values of *LA* and PSA, 10-fold were selected at random

208   with replacement, each fold containing 36 paired values (i.e. 80% of the total) on which the

209   model was trained. The remaining 20% was used for testing purposes.

210   According to Diago et al. (2012) the *LA'* model was then validated using another set of

211   grapevine RGB images collected on additional 16 vines and its accuracy determined

212   through the correlation coefficient R^2 between actual leaf area and *LA'*.

213

214   Evolution of *LA'* in each irrigation treatment was non-destructively determined via imaging

215   using the same 4-5 individual vines per irrigation treatment at 0, 3, 6, 9, 11, 14, 19, and 22

216   DADI and calculating the mean PSA per treatment through eq. 1.

217

218   *2.6 Specific vine water consumption*

219   On the same vine used for Ψ determination the vine water consumption was determined by

220   weighing the pots every evening. The weight of the previous day was used as a reference

221   to determine daily water loss from each plant. Then values were normalised per unit of *LA'*

222   and reported as g H_2O cm^{-2} d^{-1}.

223

224

225   *2.7 Data analysis*

226   The statistical analysis was performed using R software (3.3.2 version) package 'agricolae'

227   (de Mendiburu, 2016), plotting and fitting were by OriginPro 9.3 (OriginLab Corporation,

228   USA). Data were reported as mean and standard error of the mean ($\pm$SE). A one-way

229   ANOVA was used to examine the differences between irrigation treatments at each

230   sampling date, the differences among means were identified by Tukey Honest Significance

231   Difference (HSD) post-hoc tests; *p* values <0.05 were considered significant.

232

233   **3. Results and discussion**

234   This study was carried out at a robotised plant phenotyping platform and examined the

235   influence of vine water status (as assessed through Ψ) on simultaneously physiological and

236   phenomic traits of grapevine expanding knowledge on HTP tools for vine performance

237   assessment *sensu* Großkinsky et al. (2015).

238

239   *3.1 Physiological and morphometric drought response*

240   Soil moisture in well watered pots was stable around 35% dw during the experiment, while

241   it progressively declined in drought stressed pots from the 3rd DADI becoming significantly

242   different from that of control ones by 11 DADI (Fig. 2). At the end of experiment, soil

243   moisture reached values close to 10% (*IRR*$_{25\%}$), 14% (*IRR*$_{50\%}$) and 21% (*IRR*$_{75\%}$) (Fig. 2).

244   Such soil moisture variation among treatments is similar to that observed by Sivilotti et al.

245   (2005) in a pot experiment. .Values of Ψ_{PD} ranged from approx. -0.2 (control vine) to a

246   minimum of approx. -0.8 ($IRR_{50\%}$) and -1.15 MPa ($IRR_{25\%}$) detected at 22 DADI, while in

247   vines receiving 75% of daily water consumption Ψ_{PD} remained close to -0.2 MPa

248   throughout the experiment similarly to that of control vines (Fig. 3).

249   When measured at midday, Ψ reveals the sign of drought imposition at 11 DADI as at this

250   stage the Ψ_{MD} of various treatments differed significantly from that of control while at the

251   same day the Ψ_{PD} was significantly differentiated only for the $IRR_{25\%}$ treatment (Fig. 3).

252   Hence, it appears that Ψ_{MD} is more informative than Ψ_{PD} in revealing changes in vine water

253   status at least under the present experimental conditions.

254   From the 11st DADI onward Ψ_{MD} further decreased reaching the lowest value in $IRR_{25\%}$ (-

255   1.3 MPa) at the last day of the experiment when both $IRR_{50\%}$ and $IRR_{75\%}$ were close to -1

256   MPa (Fig. 3). For the $IRR_{75\%}$ treatment, the amount of water restored each day allowed an

257   over-night recovery of plant water status as documented by their Ψ_{PD} that approached the

258   values of well irrigated vines. Likely a longer or drier drought period would be required to

259   induce a significant decline of Ψ_{PD} in $IRR_{75\%}$ compared to control vine..

260

261   Both Ψ_{PD} and Ψ_{MD} patterns recall similar trends previously observed in grapevines

262   subjected to water stress (Poni et al., 2014). Despite this being an "in-pot experiment",

263   based on the trends of Ψ the water withhold procedure should be considered slow enough

264   to let vines to adapt to soil moisture depletion in terms of drought related changes to leaf

265   water content and pigments (e.g., chlorophyll, xanthophylls) which may influence leaf

266   reflectance (Palliotti et al., 2015).

267   The level of net photosynthetic rate recorded in well irrigated vines was similar to that of 6-

268   8-year old field grown grapevines (Chaves et al., 2010) oscillating around the mean value

269   of 12.3 μmol CO_2 m^{-2} s^{-1} throughout the experiment (Fig. 4A). Drought-induced variations

270   of *A* were considerably in accordance with that of g_s, however for the $IRR_{25\%}$ group the

271   initial decline of *A* detected within the early 11 DADI was more smooth than that of g_s (Fig.

272   4A and C). This was likely due to an improved intrinsic water use efficiency occurred for

273   the most drought stressed treatment (Poni et al., 2007).

274

275   Leaf transpiration in well irrigated grapevines ranged from 3.8 (6 DADI) to 9.9 mmol H_2O

276   m^{-2} s^{-1} (22 DADI) (Fig. 4B) mainly due to changes in *VPD* that peaked at ~2 and ~4 kPa at

277   6 and 22 DADI, respectively (Fig. 5). Particularly, at the beginning of drought imposition

278   (between 6 and 11 DADI) values of *E* for control, $IRR_{75\%}$ and $IRR_{50\%}$ treatments transiently

279   declined because of lower *VPD* (Fig. 5). On average maximum air temperature ranged from

280   approx. 26 to 28 °C even though it was 3-4°C lower at 0, 6, 8 and 20 DADI, maximum

281   midday irradiance level was always above 1,000 μmol m^{-2} s^{-1} PAR is day 8 and 20 DADI

282   are excepted (Fig. 5).

283

284   The differences in leaf transpiration detected among treatments reflect a typical down-

285   regulated behaviour of *E* dependent upon the imposed irrigation treatment (Fig. 4B)

286   (Medrano et al., 2003).

287   Stomatal conductance in well irrigated grapevines was stable at approx. 0.3 mol H_2O m^{-2} s^{-}

288   ^{1} throughout the experiment excepting a transient decrease at 11 DADI (Fig. 4C). In

289   severely drought stressed grapevines ($IRR_{25\%}$) the g_s significantly declined after the 3rd

290   DADI and it sharply reached a value ~80% lower than that of control vines at 6 DADI.

291   Thereafter the g_s of $IRR_{25\%}$ further declined toward the minimum value reached by 11

292   DADI where it remained until the end of the experiment (Fig. 4C).

293   The influence of reduced irrigation on g_s was similar for $IRR_{50\%}$ and $IRR_{75\%}$ showing a

294   gradual reduction during the early 10 DADI when a g_s value of ~35% of that of well

295   irrigated was reached (Fig. 4C). During the remaining period of the experiment (from 11 to

296   22 DADI) g_s values recorded in $IRR_{75\%}$ grapevines were approx. 40% of that of control

297   ones, while in $IRR_{50\%}$ vines the g_s was similar to that of $IRR_{25\%}$ ones (Fig. 4C) remaining

298   below the threshold of 0.05 mol H_2O m^{-2} s^{-1} that identifies severe drought condition *sensu*

299   Cifre et al. (2005).

300

301   Interpretation of leaf gas exchange variations induced by different irrigation supply should

302   also include the variations of plant water status in order to comprehensively argue key

303   drought-related physiological issues and allow a wider usefulness of data. Hence, here leaf

304   gas exchanges are also discussed in parallel with Ψ_{MD} allowing construction of a more

305   comprehensive data set to potentially be associated to vine phenotyping.

306

307   The decline of g_s was able to regulate leaf transpiration and net photosynthetic rate across

308   the Ψ_{MD} range recorded (Fig. 6A, B) confirming water loss and carbon gain mechanisms

309   observed in drought stressed grapevines (Medrano et al., 2003). The reduction of g_s

310   determined by drought imposition followed the changes of Ψ_{MD} (Fig. 6C) accordingly to

311   similar correlative information reported for both pot and open-field studies (Medrano et al.,

312   2003; Cifre et al., 2005). In this study the efficiency of the PSII was not impaired by the

313   drought imposition as suggested by the stable chlorophyll fluorescence (F_v/F_m) recorded

314   throughout the experiment which were independent of the Ψ changes (Fig. 6D). That is,

315   values of F_v/F_m measured across the approx. -0.15/-1.5 MPa range of Ψ remained close to

316   0.8 (Fig. 6D) which is believed the threshold for efficient PSII indicating that the reduction

317   of net photosynthetic rates detected in drought stressed vines (Fig. 4A) was not metabolic

318   as discussed in Montanaro et al. (2009). Hence, the unchanged F_v/F_m despite the worsening

319   of Ψ confirms that fluorescence-based HTP has some limitations for the detection of water

320   stress (Berger et al., 2010).

321

322   Estimation of grapevine *LA* through non-destructive techniques has been the subject of

323   several HTP studies mainly devoted to segmentation of various plant organs (e.g., bunch,

324   leaf) for crop monitoring and breeding purposes (Diago et al., 2012; Costa et al., 2016). The

325   present study expands information on *LA* estimation in grapevines subjected to various

326   irrigation treatments being potentially useful at least in plant phenotyping platforms

327   contributing to the definition of *"standard conditions"* (Pieruschka and Hendrik, 2012).

328   In order to continuously evaluate the impact of drought on vegetation development and in

329   turn on vine water consumption a RGB-based methodology was implemented to estimate

330   the growth of leaf area which is a morphometric trait intimately related to soil moisture and

331   Ψ (Koundouras et al., 2008).

332   Results show that the actual leaf area of vines and the number of pixels corresponding to

333   the leaf surface determined through eq. 1 were linearly correlated ($R^2 = 0.78$) (Fig. 7). The

334   resulting linear model (y = 416.11 +0.915 × PSA) was capable to predict ($R^2 = 0.92$) the

335   leaf area of a different set of grapevines ($n = 16$) (see the inset in Fig. 7). The cross-

336   validated estimation of *LA* performed in this study consisted of data collected from vines

337   under various irrigation levels improving previous similar models (e.g., Diago et al. 2012).

338

339   The *LA'* of various irrigation treatments was not influenced early after drought application

340   (Fig. 8). At day 11 DADI, some significant differences were envisaged at least between

341   *IRR*$_{75\%}$ and the more severely drought stressed vines (*IRR*$_{25\%}$) (Fig. 8), unfortunately *LA'*

342   data for well irrigated vines were not available due to technical difficulties. Thereafter,

343   control vine canopies showed significantly higher values than that of *IRR*$_{25\%}$ and tend to be

344   higher than that of *IRR*$_{75\%}$ however differences were not always significant. At the end of

345   the experimental period *LA'* in well irrigated vines increased by approx. 85% of the initial

346   value, while *IRR*$_{75\%}$ vines consistently showed a growth as low as ∼45% of the initial *LA'*

347   (Fig. 8). The *IRR*$_{25\%}$ and *IRR*$_{50\%}$ treatments had their highest *LA'* increased similarly by

348   approx. 20% of the initial value at 19 DADI (Fig. 8). However, *LA'* was 6-9% at the end of

349   experiment likely due to a sharp leaf fall triggered by the severe drought (Munné-Bosch

350   and Alegre, 2004).

351

352   The slowdown of leaf growth in grapevines under drought is an adaptive trait (Poni et al.,

353   2007) which was non-destructively detected in this study through the modelled leaf area

354   allowing the identification of paired vine groups according to their Ψ_{PD} (i.e., control

355   coupled with *IRR*$_{75\%}$ *versus IRR*$_{50\%}$ coupled with *IRR*$_{25\%}$).

356   This study was not designed to detect the growth responses of various vegetative

357   components (e.g., shoot, leaf) (see Pellegrino et al., 2008). However, results on the

358   influence of water shortage on the overall leaf area growth are consistent with those

359   reported by Gómez-del-Campo et al. (2002) for a similar experiment that was conducted

360   using larger pots (35 L). Lanari et al., (2015) report a ~70% reduced leaf area (destructively

361   determined) in potted (4 L) grapevines receiving 40% of full irrigation after 18 DADI. In

362   the present experiment, leaf area in *IRR*$_{25\%}$ vines was 40% lower than control 22 DADI

363   when Ψ_{MD} was -1.3 MPa (Fig. 3 and 8), unfortunately data on Ψ are not provided by Lanari

364   et al., (2015) making deep comparisons challenging.

365

366   The estimated leaf area was involved in the determination of daily water consumption

367   which was on average 0.16 g H_2O cm^{-2} d^{-1} in well irrigated vines and in drought stressed

368   ones at the beginning of the experiment when Ψ_{MD} was in the -0.5/-0.3 MPa region,

369   thereafter it declined by 85% when Ψ_{MD} reached -1.2 MPa (Fig. 9). Such a reduction is

370   comparable to that reported by Medrano et al. (2012) for non-irrigated, field grown

371   grapevines. Results show that specific water consumption responded to the drought-

372   induced decline of Ψ_{MD} following an exponential decay pattern (R^2 =0.86) (Fig. 9)

373   suggesting it might be a promising HTP tool for both plant water status and consumption

374   determination. In addition, considering that values of vine water consumption were

375   calculated on a vine basis (see Method section) it might support the calculation of some

376   functional traits at vine scale (e.g., water use efficiency) thus avoiding criticisms related to

377   their single-leaf assessment (Poni et al., 2014).

378

379   *3.2 RGB and NIR response to drought*

380   The RGB images sourced by Visible light cameras have great potential for morphological

381   studies including leaf area estimation as shown in this study, nevertheless they are known

382   to have some limitations in serving as a proxy for plant physiological traits (Großkinsky et

383   al. 2015). The relatively weak correspondence between Ψ and some specific RGB colour

384   class obtained in the present research partly supports that conclusion. That is, the Brown

385   and Green colours data showed a poor correlation with Ψ as indicated by the values of R^2 of

386   0.24 and 0.04, respectively (Fig. 10A, 10B). However, an improved correlation was

387   achieved considering the Yellow colour class whose fraction linearly increased with

388   lowering Ψ ($R^2 = 0.5$) when vines becoming more stressed (Fig. 10C). The yellowing of

389   foliage is a regulatory process leading to leaf senescence in response to ageing or

390   environmental stresses including drought (Munné-Bosch and Alegre, 2004). Recently, the

391   yellowing (or the loss of greenness) of leaf has been discussed as a promising digital tool

392   for identification of drought resistant (or sensitive) annual crops (e.g., rice and sorghum)

393   (Harris et al., 2017; Lingfeng et al., 2018). This supports the interpretation of the increasing

394   Yellow fraction being related to increasing drought (i.e., more negative Ψ) (Fig. 10C).

395   Interestingly, the fraction of the Dark Green colour class showed the highest correlation

396   with Ψ reaching $R^2 = 0.71$ (Fig. 10D). Such a close correspondence between reducing

397   pattern of the Dark Green colour class under increasing drought might be explained

398   considering the putative increased leaf angle and in turn the increased exposure of the

399   abaxial (lower) leaf surface occurring with drought. It makes sense to remember that the

400   abaxial surface has a lighter colour compared to the adaxial (upper) one due to the presence

401   of trichomes (Boso et al., 2010 and references therein).

402   Increased leaf lamina angle is among the plant drought defence mechanisms activated for

403   PSII and water conservation reducing direct insolation and in turn temperature,

404   conductance and transpiration of leaf (Palliotti et al., 2008; Jones et al., 2009). Incidentally,

405   the stable F_v/F_m values recorded in well irrigated and drought stressed vines (Fig. 6D)

406   might conceivably be associated with the protective increased leaf angle (i.e., leaf tends to

407   be more vertical) in drought stressed leaves that most probably had occurred (Chaves et al.,

408   2010). Inclination of leaf petiole from the vertical axis in grapevine might increase from

409   60-70° in well irrigated vines up to 120° in drought stressed ones (approx. -1.8 MPa, early

410   morning) (Nuzzo, pers. com.). This interpretation is in line with the idea that some RGB

411   images are useful to track morphological changes (Großkinsky et al. 2015), however the

412   causal chain *"drought→increased leaf angle→reduced Dark Green fraction"* deserves

413   further study.

414

415   The change of relative water content in leaf (i.e., the percentage of water present at the time

416   of sampling, relative to the amount of water in a saturated leaf) is a reliable index of plant

417   water status that linearly and closely correlates with Ψ in several species including *Vitis*

418   (Smart and Bingham, 1974; Bota et al., 2004). Relative leaf water content is known as the

419   most prominent parameter influencing leaf spectral reflectance and therefore non-

420   destructively technologies including those based on NIR wavelengths, which are useful for

421   plant water status monitoring (Seelig et al., 2008; Berger et al., 2010; Diago et al., 2018).

422   Recently, the Ψ in grapevines subjected to drought has been modelled using portable NIR

423   equipment to record diffuse reflectance spectra of the leaf surfaces by means of contact

424   probes (De Bei et al., 2011; Tardaguila et al., 2016). Rapaport et al. (2015) combine

425   information on spectral signatures collected with both portable spectrometer and cameras

426   equipped with specific narrow-band filters to model Ψ at canopy level using a set of 4-leaf

427   images. In the present study a contactless and image-based methodology has been used to

428   collect NIR colour class at plant canopy scale which were correlated with Ψ ($R^2 = 0.44$)

429   even if a certain variability of NIR reflectance at a specific Ψ remain (Fig. 11). The

430   potential influence on NIR reflectance exerted by other leaf traits linked to decreasing leaf

431   water content such as leaf thickness (Seelig et al., 2008) and different signature of abaxial

432   and adaxial surface (see discussion above) might help to explain such a variability. Results

433   confirm the potential suitability of NIR colour class to be a proxy of Ψ within affordable

434   phenotyping,   however   hyperspectral   whole-canopy   image-based   NIR   reflectance

435   measurements in drought phenotyping studies might further strength the relationship

436   between Ψ and NIR signatures in grapevines (Diago et al., 2017; Berger et al., 2010).

437   This study reports correlative information between physiological traits and image-based

438   HTP analysis for grapevines experiencing water shortage at a robotised plant phenotyping

439   platform   which   is   part   of   the   EPPN   (*European   Plant   Phenotyping   Network*,

440   *https://eppn2020.plant-phenotyping.eu/EPPN2020_home*).   EPPN   and   the   global

441   phenotyping community are doing efforts toward the standardisation of phenotyping

442   protocols offering training in HTP, broaden access to shared-usage HTP facilities,

443 developing common data storage and standards for the design, analysis, and reporting of

444 HTP data sets (van Eeuwijk et al., 2018).

445

446 **4. Conclusions**

447 This study documents the suitability of the Dark Green fraction of the RGB spectrum to be

448 a proxy for a relatively wide range of Ψ (from -0.2 down to -1.6 MPa) which would suggest

449 a new study with the working hypothesis that leaf lamina (or petiole) angle can act as a

450 HTP drought-induced trait. The monitoring of the *LA'* evolution in vines under various

451 drought levels might be a promising HTP tool to identify occurrence of water-stress

452 combining both morphometric (leaf area) and physiological (water consumption) responses.

453 RGB and NIR sensors have been used in this study confirming that easily accessible

454 sensors might support possible implementation of affordable phenotyping (*sensu* Reynolds

455 et al., 2018) and assist in developing new tools for precision irrigation in a HTP domain.

456 The parallel results on leaf gas exchange, plant water status and on efficiency of PSII

457 collected along with RGB and NIR images under known environmental conditions might

458 collectively favour the standardisation of phenotyping protocols.

459

465

Acknowledgements

467   Authors thank Mr A. Mossuto (Natura Informatica Soc. Coop.) for technical assistance.

468

References

470   Acevedo-Opazo, C., Ortega-Farias, S., Fuentes, S., 2010. Effects of grapevine (*Vitis*
471   *vinifera* L.) water status on water consumption, vegetative growth and grape quality:
472   An irrigation scheduling application to achieve regulated deficit irrigation. Agr. Water
473   Manage. 97, 956–964. https://doi.org/10.1016/j.agwat.2010.01.025.

474   Acosta-Gamboa, L. M., Liu, S., Langley, E., Campbell, Z., Castro-Guerrero, N., Mendoza-
475   Cozatl, D., & Lorence, A., 2017. Moderate to severe water limitation differentially
476   affects the phenome and ionome of Arabidopsis. Funct Plant Biol, 44(1), 94-106.

477   Arvidsson S, Pérez-Rodríguez P, Mueller-Roeber B., 2011. A growth phenotyping pipeline
478   for Arabidopsis thaliana integrating image analysis and rosette area modeling for
479   robust quantification of genotype effects. New Phytol, 191, 895–907.
480   doi:10.1111/j.1469-8137.2011. 03756.x

481   Balafoutis, A., Beck, B., Fountas, S., Vangeyte, J., van der Wal, T., Soto-Embodas, I.,
482   Gomez-Barbero, M.,   Barnes, A.P., Eory, V. 2017. Precision Agriculture
483   Technologies positively contributing to GHG emissions mitigation, farm productivity
484   and economics. Sustainability 9(8), 1339.

485   Bellvert J, Zarco-Tejada PJ, Marsal J, Girona J, González-Dugo V, Fereres E., 2016
486   Vineyard irrigation scheduling based on airborne thermal imagery and water potential
487   thresholds. Aust J Grape Wine R, 22(2):307–315.

488   Berger, B., Parent, B., Tester, M., 2010. High-throughput shoot imaging to study drought
489   responses. J. Exp. Bot. 61, 3519–3528. https://doi.org/10.1093/jxb/erq201

490   Black C.A. 1965. Methods of Soil Analysis: Part I Physical and mineralogical properties.
491   American Society of Agronomy, Madison, Wisconsin, USA.

492   Boso, S., Alonso-Villaverde, V., Santiago, J.L., Gago, P., Dürrenberger, M., Düggelin, M.,
493   Kassemeyer, H.H., Martinez, M.C., 2010. Macro- and microscopic leaf characteristics
494   of six grapevine genotypes (*Vitis* spp.) with different susceptibilities to grapevine
495   downy mildew. Vitis 49(1), 43-50.

496   Bota, J., Medrano, H., Flexas, J., 2004. Is photosynthesis limited by decreased Rubisco
497   activity and RuBP content under progressive water stress? New Phytol. 162, 671–681.
498   https://doi.org/10.1111/j.1469-8137.2004.01056.x

499   Casadesús J, Kaya Y, Bort J, Nachit MM, Araus JL, Amor S, et al., 2017. Using vegetation
500   indices derived from conventional digital cameras as selection criteria for wheat
501   breeding in water-limited environments. Ann App Biol,150(2):227–36.

502   Chaves, M.M., Zarrouk, O., Francisco, R., Costa, J.M., Santos, T., Regalado, A.P.,
503   Rodrigues, M.L., Lopes, C.M., 2010. Grapevine under deficit irrigation: hints from
504   physiological and molecular data. Ann. Bot. 105, 661–676.
505   https://doi.org/10.1093/aob/mcq030

506   Cifre, J., Bota, J., Escalona, J.M., Medrano, H., Flexas, J., 2005. Physiological tools for
507   irrigation scheduling in grapevine (Vitis vinifera L.). Agric. Ecosyst. Environ. 106,
508   159–170. https://doi.org/10.1016/j.agee.2004.10.005

509   Cohen Y, Alchanatis V, Sela E, Saranga Y, Cohen S, Meron M, et al. 2015. Crop water
510   status estimation using thermography: Multi-year model development using ground-
511   based thermal images. Precis Agric, 16(3):311–329.

512   Costa, J.M., Vaz, M., Escalona, J., Egipto, R., Lopes, C., Medrano, H., Chaves, M.M.,
513   2016. Modern viticulture in southern Europe: Vulnerabilities and strategies for
514   adaptation to water scarcity. Agric Water Manag 164, 5–18.
515   https://doi.org/10.1016/j.agwat.2015.08.021

516   De Bei, R., Cozzolino, D., Sullivan, W., Cynkar, W., Fuentes, S., Dambergs, R., Pech, J.,
517   Tyerman, S., 2011. Non-destructive measurement of grapevine water potential using
518   near infrared spectroscopy: Measure of grapevine water potential using NIR. Aust. J.
519   Grape Wine R. 17, 62–71. https://doi.org/10.1111/j.1755-0238.2010.00117.x

520   de Mendiburu F., 2016. Agricolae: Statistical procedures for agricultural research. R
521   package version 1.2-4. https://CRAN.R-project.org/package=agricolae

522   Diago, M.P., Bellincontro, A., Scheidweiler, M., Tardaguila, J., Tittmann, S., Stoll, M.,
523   2017. Future opportunities of proximal near infrared spectroscopy approaches to
524   determine the variability of vineyard water status. Aust J Grape Wine R 23, 409-414.

525   Diago, M.-P., Correa, C., Millán, B., Barreiro, P., Valero, C., Tardaguila, J., 2012.
526   Grapevine Yield and Leaf Area Estimation Using Supervised Classification
527   Methodology on RGB Images Taken under Field Conditions. Sensors 12, 16988–
528   17006. https://doi.org/10.3390/s121216988

529 Diago, M.P., Fernández-Novales, J., Gutiérrez, S., Marañón, M., Tardaguila, J., 2018
530   Development and validation of a new methodology to assess the vineyard water status
531   by on the go near infrared spectroscopy. Frontiers Plant Sci 9, 59.

532 Doorenbos, J. and Pruitt, W. O., 1977. Crop water requirements. Irrigation and Drainage
533   Paper No. 24, FAO, Rome, Italy.

534 Duan Lingfeng, Han Jiwan, Guo Zilong, Tu Haifu, Yang Peng, Zhang Dong, Fan Yuan,
535   Chen Guoxing, Xiong Lizhong, Dai Mingqiu, Williams Kevin, Corke F., Doonan
536   J.H., Yang W., 2018. Novel digital features discriminate between drought resistant
537   and drought sensitive rice under controlled and field conditions. Frontiers in Plant
538   Science 9, 492. doi=10.3389/fpls.2018.00492

539 Fernández, J.E., 2017. Plant-based methods for irrigation scheduling of woody crops.
540   Horticulturae 3, 35, doi:10.3390/horticulturae3020035.

541 Fernández-Novales, J., Tardaguila, J., Gutiérrez, S., Marañón, M., Diago, M.P., 2018. In
542   field quantification and discrimination of different vineyard water regimes by on-the-
543   go NIR spectroscopy. Biosyst Eng 165, 47-58.

544 Fiorani, F., and Schurr, U. (2013). Future scenarios for plant phenotyping. Annu. Rev.
545   Plant. Biol. 64, 267–291.

546 Flexas, J., Escalona, J.M., Medrano, H., 1998. Down-regulation of photosynthesis by
547   drought under field conditions in grapevine leaves. Funct. Plant Biol. 25, 893–900.
548   https://doi.org/10.1071/pp98054.

549 Gago, J., Fernie, A.R., Nikoloski, Z., Tohge, T., Martorell, S., Escalona, J.M., Ribas-Carbó,
550   M., Flexas, J., Medrano, H., 2017. Integrative field scale phenotyping for
551   investigating metabolic components of water stress within a vineyard. Plant Methods
552   13. https://doi.org/10.1186/s13007-017-0241-z

553 Ge, Y., Bai, G., Stoerger, V., Schnable, J.C., 2016. Temporal dynamics of maize plant
554   growth, water use, and leaf water content using automated high throughput RGB and
555   hyperspectral imaging. Comput. Electron. Agr. 127, 625–632.
556   https://doi.org/10.1016/j.compag.2016.07.028

557 Girona, J., Mata, M., del Campo, J., Arbonés A., Bartra E., Marsal J., 2006. The use of
558   midday leaf water potential for scheduling deficit irrigation in vineyards. Irrig. Sci.
559   24, 115-127. https://doi.org/10.1007/s00271-005-0015-7.

560 Gomez-del-Campo M., Ruiz C., Lissarrague J.R., 2002. Effect of water stress on leaf area
561   development, photosynthesis, and productivity in Chardonnay and Airén grapevines.
562   Am. J. Enol. Vitic. 53(2),138-143

563   Goudriaan J., van Laar H.H. (1994). Modelling potential crop growth processes. Kluwer,
564   Dordrecht.

565   Grant OM, Tronina Ł, Jones HG, Chaves MM. Exploring thermal imaging variables for the
566   detection of stress responses in grapevine under different irrigation regimes. J. Exp
567   Bot 2007;58(4):815–825.

568   Großkinsky, D.K., Svensgaard, J., Christensen, S., Roitsch, T., 2015. Plant phenomics and
569   the need for physiological phenotyping across scales to narrow the genotype-to-
570   phenotype knowledge gap. J. Exp. Bot. 66, 5429–5440.
571   https://doi.org/10.1093/jxb/erv345

572   Gutiérrez, S., Diago, M.P., Fernández-Novales, J., Tardaguila, J.,2018. Vineyard water
573   status assessment using on-the-go thermal imaging and machine learning. PLOS One
574   13(2), e0192037. DOI: 10.1371/journal.pone.0192037

575   Hairmansis, A., Berger, B., Tester, M., Roy, S.J., 2014. Image-based phenotyping for non-
576   destructive screening of different salinity tolerance traits in rice. Rice 7, 16.
577   https://doi.org/10.1186/s12284-014-0016-3.

578   Harbinson, J.; Prinzenberg, A.E.; Kruijer, W.; Aarts, M.G. High throughput screening with
579   chlorophyll fluorescence imaging and its use in crop improvement. Curr. Opin.
580   Biotechnol. 2012, 23, 221–226.

581   Harris K., Subudhi PK, Borrell B., Jordan D., Rosenow D., Nguyen H., Klein P., Klein R.,
582   Mullet J., 2017. Sorghum stay-green QTL individually reduce post-flowering
583   drought-induced leaf senescence. J. Exp. Bot. 58 (2), 327–338,
584   https://doi.org/10.1093/jxb/erl225

585   Herrero-Langreo, A., Tisseyre, B., Roger, J.M., and Scholasch, T., 2018. Test of sampling
586   methods to optimize the calibration of vine water status spatial models. Precision
587   Agric. 19, 365–378.

588   IPCC, 2013: Climate Change 2013: The Physical Science Basis. Cambridge University
589   Press, 1535 pp., doi:https://doi.org/10.1017/CBO9781107415324.

590   Jones, H.G., Serraj, R., Loveys, B.R., Xiong, L., Wheaton, A., Price, A.H., 2009. Thermal
591   infrared imaging of crop canopies for the remote diagnosis and quantification of plant
592   responses to water stress in the field. Funct. Plant Biol. 36, 978.
593   https://doi.org/10.1071/FP09123

594   Kassemeyer, H. H., Martinez, M. C., 2010. Macro- and microscopic leaf characteristics of
595   six grapevine genotypes (*Vitis* spp.) with different susceptibilities to grapevine downy
596   mildew. Vitis 49 (1), 43–50.

597   Koundouras, S., Tsialtas, I.T., Zioziou, E., Nikolaou, N., 2008. Rootstock effects on the
598   adaptive strategies of grapevine (Vitis vinifera L. cv. Cabernet–Sauvignon) under
599   contrasting water status: Leaf physiological and structural responses. Agric. Ecosyst.
600   Environ. 128, 86–96. https://doi.org/10.1016/j.agee.2008.05.006

601   Lanari, V., Silvestroni, O., Palliotti, A., Green, A., Sabbatini, P., 2015. Plant and Leaf
602   Physiological Responses to Water Stress in Potted 'Vignoles' Grapevine. Hort Sci.
603   50, 1492–1497.

604   Lichtenberg, E., J. Majsztrik, M. Saavoss (2015). Grower demand for sensor-controlled
605   irrigation. Water Resour. Res., 51, 341–358, doi:10.1002/2014WR015807

606   Maxwell K. and Johnson G.N. (2000). Chlorophyll fluorescence—a practical guide. J. Exp.
607   Bot. 51, 659–668.

608   Medrano, H., Escalona, J.M., Cifre, J., Bota, J., Flexas, J., 2003. A ten-year study on the
609   physiology of two Spanish grapevine cultivars under field conditions: effects of water
610   availability from leaf photosynthesis to grape yield and quality. Funct. Plant Biol. 30,
611   607. https://doi.org/10.1071/FP02110

612   Medrano, H., Pou, A., Tomás, M., Martorell, S., Gulias, J., Flexas, J., Escalona, J.M., 2012.
613   Average daily light interception determines leaf water use efficiency among different
614   canopy locations in grapevine. Agric. Water Manag. 114, 4–10.
615   https://doi.org/10.1016/j.agwat.2012.06.025

616   Miller, S. A., Smith G. S., Boldingh H. L., Johansson A., 1998. Effects of water stress on
617   fruit quality attributes of kiwifruit. Ann. Bot. 81, 73-81.

618   Montanaro, G., Dichio, B., Xiloyannis, C., 2009. Shade mitigates photoinhibition and
619   enhances water use efficiency in kiwifruit under drought. Photosynthetica 47(3), 363-
620   371.

621   Mulla, D.J., 2013. Twenty-five years of remote sensing in precision agriculture: Key
622   advances and remaining knowledge gaps. Biosyst. Engi. 114 (4). 358-371.
623   https://doi.org/10.1016/j.biosystemseng.2012.08.009.

624   Munné-Bosch, S., Alegre, L., 2004. Die and let live: leaf senescence contributes to plant
625   survival under drought stress. Funct. Plant Biol. 31, 203–216.
626   https://doi.org/10.1071/fp03236.

627   Palliotti, A., Silvestroni, O., Petoumenou, D., Vignaroli, S., Berrios, J.G., 2008. Evaluation
628   of low-energy demand adaptive mechanisms in Sangiovese grapevine during drought.
629   1 42, 41–47. https://doi.org/10.20870/oeno-one.2008.42.1.832.

630   Palliotti, A., Tombesi, S., Frioni, T., Silvestroni, O., Lanari, V., D'Onofrio, C., Matarese,
631   F., Bellincontro, A., Poni, S., 2015. Physiological parameters and protective energy

632   dissipation mechanisms expressed in the leaves of two Vitis vinifera L. genotypes

633   under multiple summer stresses. J. Plant Physiol.185, 84–92.

634   https://doi.org/10.1016/j.jplph.2015.07.007.

635 Pellegrino A., Lebon E., Simonneau T., Wery J., 2008. Towards a simple indicator of water

636   stress in grapevine (Vitis vinifera L.) based on the differential sensitivities of

637   vegetative growth components. Aust. J. Grape Wine Res. 11(3): 306-315.

638 Petrozza, A., Santaniello, A., Summerer, S., Di Tommaso, G., Di Tommaso, D., Paparelli,

639   E., Piaggesi, A., Perata, P., Cellini, F., 2014. Physiological responses to Megafol®

640   treatments in tomato plants under drought stress: A phenomic and molecular

641   approach. Sci. Hort. 174, 185–192. https://doi.org/10.1016/j.scienta.2014.05.023.

642 Poblete, T., Ortega-Farías, S., Moreno, M., Bardeen, M., 2017. Artificial Neural Network

643   to Predict Vine Water Status Spatial Variability Using Multispectral Information

644   Obtained from an Unmanned Aerial Vehicle (UAV). Sensors 17, 2488.

645   https://doi.org/10.3390/s17112488

646 Poni S., Bernizzoni F., Civardi S., 2007. Response of "Sangiovese" grapevines to partial

647   root-zone drying: Gas-exchange, growth and grape composition. Sci. Hortic. 114(2),

648   96-103.

649 Poni, S., Galbignani, M., Magnanini, E., Bernizzoni, F., Vercesi, A., Gatti, M., Merli, M.C.,

650   2014. The isohydric cv. Montepulciano (*Vitis vinifera* L.) does not improve its whole-

651   plant water use efficiency when subjected to pre-veraison water stress. Sci. Hortic.

652   179, 103–111. https://doi.org/10.1016/j.scienta.2014.09.021

653 Rapaport, T., Hochberg, U., Shoshany, M., Karnieli, A., Rachmilevitch, S., 2015.

654   Combining leaf physiology, hyperspectral imaging and partial least squares-

655   regression (PLS-R) for grapevine water status assessment. ISPRS J. Photogramm.

656   109, 88–97. https://doi.org/10.1016/j.isprsjprs.2015.09.003

657 Reynolds, D., Baret, F., Welcker, C., Bostrom, A., Ball, J., Cellini, F., Lorence, A.,

658   Chawade, A., Khafif, M., Noshita, K., Mueller-Linow, M., Zhou, J., Tardieu, F.,

659   2018. What is cost-efficient phenotyping? Optimizing costs for different scenarios.

660   Plant Science. https://doi.org/10.1016/j.plantsci.2018.06.015

661 Rinaldi, M., He, Z., 2014. Decision support systems to manage irrigation in agriculture. In

662   Advances in Agronomy (Vol. 123, pp. 229-279). Academic Press.

663 Romero, M., Luo, Y., Su, B., Fuentes, S., 2018. Vineyard water status estimation using

664   multispectral imagery from an UAV platform and machine learning algorithms for

665   irrigation scheduling management. Comput. Electron. Agr. 147, 109–117.

666   https://doi.org/10.1016/j.compag.2018.02.013

667   Ronco, P., Zennaro, F., Torresan, S., Critto, A., Santini, M., Trabucco, A., Zollo, A.L.,
668   Galluccio, G., Marcomini, A., 2017. A risk assessment framework for irrigated
669   agriculture under climate change. Adv. Water Resour.,110, 562-578.
670   https://doi.org/10.1016/j.advwatres.2017.08.003.

671   Seelig, H.D., Hoehn, A., Stodieck, L.S., Klaus, D.M., III, W.W.A., Emery, W.J., 2008. The
672   assessment of leaf water content using leaf reflectance ratios in the visible, near-, and
673   short-wave-infrared. Int. J. Remote Sens. 29, 3701–3713.
674   https://doi.org/10.1080/01431160701772500

675   Shackel, K.A., 2007. Water relations of woody perennial plant species. J. Int. Sci. Vigne
676   Vin, 41, 121-129. https://doi.org/10.20870/oeno-one.2007.41.3.847.

677   Sivilotti P, Bonetto C, Paladin M, Peterlunger E. Effect of Soil Moisture Availability on
678   Merlot: From Leaf Water Potential to Grape Composition. Am J Enol Vitic. 2005
679   56(1):9–18.

680   Smart, R.E., Bingham, G.E., 1974. Rapid Estimates of Relative Water Content. Plant
681   Physiol. 53, 258–260. https://doi.org/10.1104/pp.53.2.258

682   Tardaguila, J., Fernández-Novales, J., Gutiérrez, S., Diago, M.P., 2017. Non-destructive
683   assessment of grapevine water status in the field using a portable NIR
684   spectrophotometer: Assessing grapevine water status using NIR. J. Sci. Food Agric.
685   97, 3772–3780. https://doi.org/10.1002/jsfa.8241

686   Turner N.C. (1981). Techniques and experimental approaches for the measurement of plant
687   water status. – Plant Soil 58: 339-366.

688   van Eeuwijk, FA, Bustos-Korts D., Emilie J. Millet, Martin P. Boer, Willem Kruijer, Addie
689   Thompson, Marcos Malosetti, Hiroyoshi Iwata, Roberto Quiroz, Christian Kuppe,
690   Onno Muller, Konstantinos N. Blazakis, Kang Yu, Francois Tardieu, Scott C.

691

692

693

694 **Figure captions**

695

696 **Fig. 1.** Schematic representation of the plant phenotyping platform showing the internal
697 distances, the track of the pot on the conveyor toward the image capture chamber (arrows);
698 the position of the irradiance (PAR), temperature and humidity sensors and the position of
699 the visible RGB and NIR chambers. A front view of the imaging chambers and conveyor is
700 reported.

701

702 **Fig. 2.** Soil moisture (% dry weight) measured during the experiment in vines receiving
703 75% (□), 50% (Δ) and 25% (○) of their daily water consumption and under control (●)
704 receiving 100%. Note that at days 0 and 3 because there were not significant differences
705 letters were not reported.

706

707 **Fig. 3.** Pattern of mean stem water potential (n= 4-5, ±SE) measured pre-dawn and midday
708 in leaves of grapevines under drought (empty symbol) receiving 75% (□), 50% (Δ) and
709 25% (○) of their daily water consumption and under control irrigation (●) receiving 100%
710 of daily water consumption. Comparison between treatments at the same time different
711 letter indicates statistically significant according to Tukey's HSD test. Note that at days 0
712 and 3 because there were not significant differences letters were not reported.

713

714 **Fig. 4.** Average values ±SE (n =4-5) of (A) net photosynthetic rate, (B) transpiration and
715 (C) stomatal conductance measured in leaves of grapevines under drought receiving 75%
716 (□), 50% (Δ) and 25% (○) of their daily water consumption and under control irrigation (●)
717 receiving 100% of daily water consumption. Bars indicate the critical HSD values
718 calculated in each sampling date (Tukey's HSD test, $p<0.05$). Note that X-axis labels were
719 positioned next to the thick to avoid overlapping.

720

721 **Fig. 5.** Diurnal variations of vapour pressure deficit (*VPD*), air temperature and irradiance
722 (PAR) recorded inside the greenhouse during the measurement days.

723

724   **Fig. 6.** Correlation between (A) leaf transpiration, (B) net photosynthetic rate, (C) stomatal

725   conductance, (D) PSII fluorescence and stem water potential measured (○) midday and (●)

726   predawn in grapevine leaves.

727

728   **Fig. 7.** Correlation between actual leaf area (y-axis) and projected shoot area (PSA)

729   calculated through eq. 1 and the resulting linear model (y = 416.11+0.915 × PSA) obtained

730   after a cross-validation analysis, the grey filled area indicate the upper and lower 95% CI

731   about the model. In the inset, predicted (*LA'*) *vs* measured leaf area (*LA*). Values of *LA'*

732   were calculated using the fitting linear equation resulting from the main plot on a different

733   set of 16 vines.

734

735   **Fig. 8.** Leaf area ($cm^2 p^{-1}$) estimated in well irrigated (black filled) and under drought (grey

736   filled) grapevines receiving 75%, 50% and 25% of their daily water consumption. Bars are

737   ±SE (*n* =4-5). Comparison of treatments at the same time different letter indicates

738   statistically significant differences (Tukey's HSD test, $p<0.05$). Note that control values at

739   day 11 were missed.

740

741   **Fig. 9.** Daily vine water consumption normalised per unit of estimated leaf area (g H_2O cm^{-2} d^{-1})

742   plotted against the stem water potential measured at midday. Note that the estimated

743   leaf area refers to *LA'* determined through the equation *LA'* = 0.915**PSA*+416.11 reported

744   in Fig. 7.

745

746   **Fig. 10.** Correlation between stem water potential and (A) Brown, (B) Green, (C) Yellow

747   fraction and (D) Dark Green classes, of the visible spectrum measured (●) pre-dawn and

748   (○) midday on canopy of potted grapevines under various water status. Note that fitting

749   lines refer to pooled midday and pre-dawn data, and that Brown and Dark Green values are

750   reported in Log_{10} scale.

751

752

753   **Fig. 11.** NIR colour class measured (●) pre-dawn and (○) midday in canopy of potted

754   grapevines under different water status. Midday and pre-dawn stem water potential data

755   were pooled before the exponential decay fitting (y = 55 + 1.1576 × X -6.5497 × X^2;

756   Levenberg Marquardt iteration algorithm)

757
758
759
760

Figure 1

Figure 2
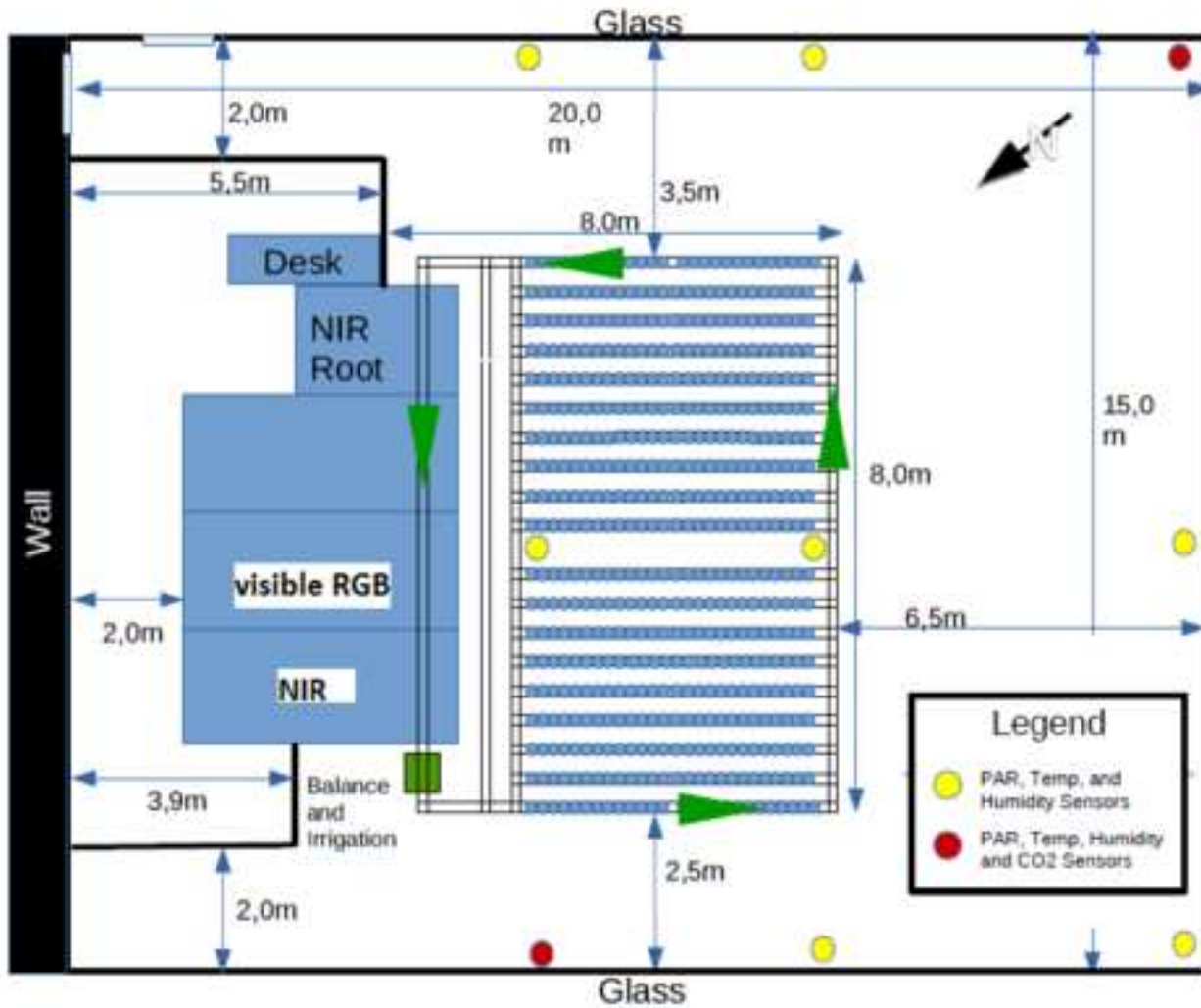**Click here to download high resolution image**
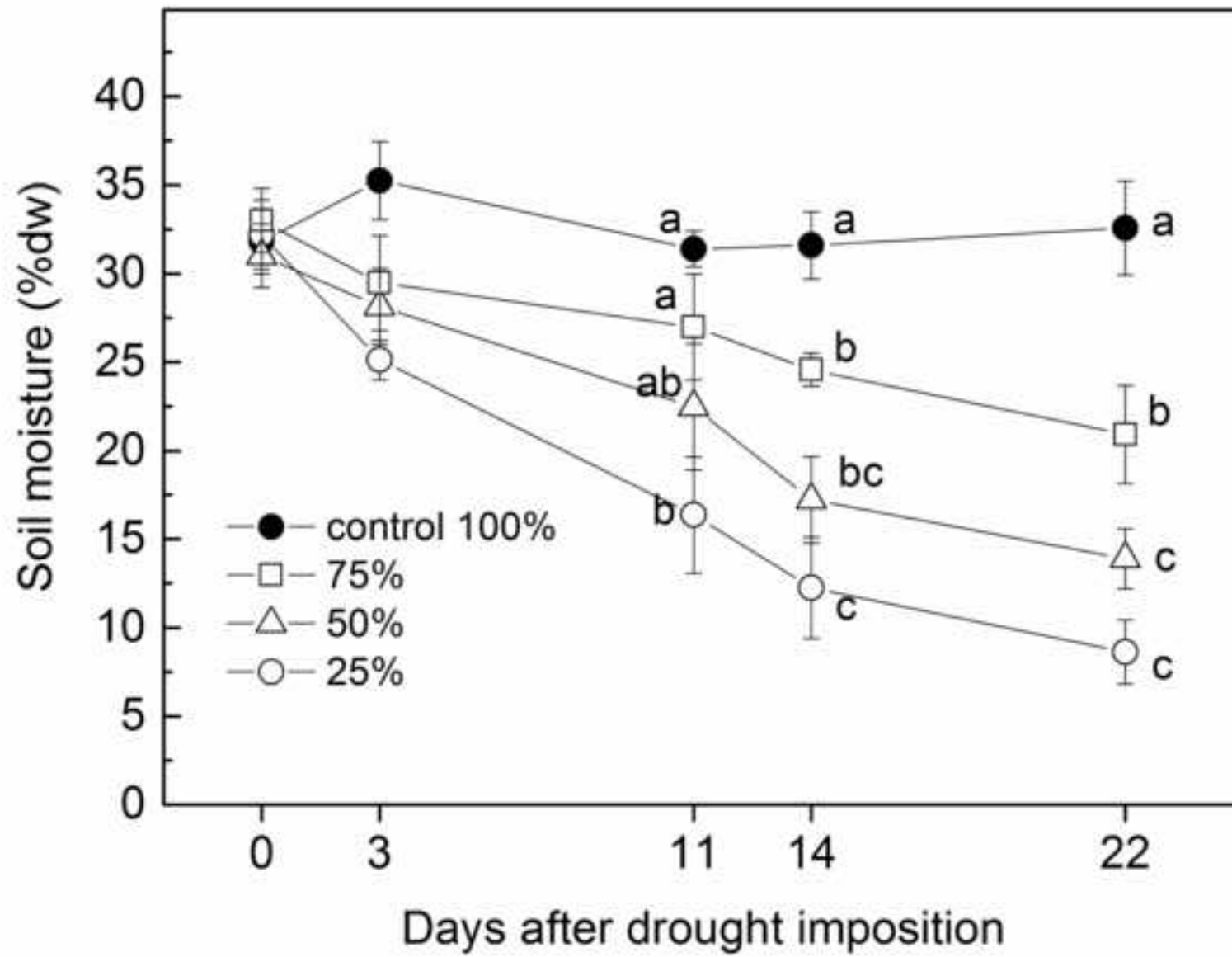
Figure 2

Figure 3
Click here to download high resolution image

Days after drought imposition
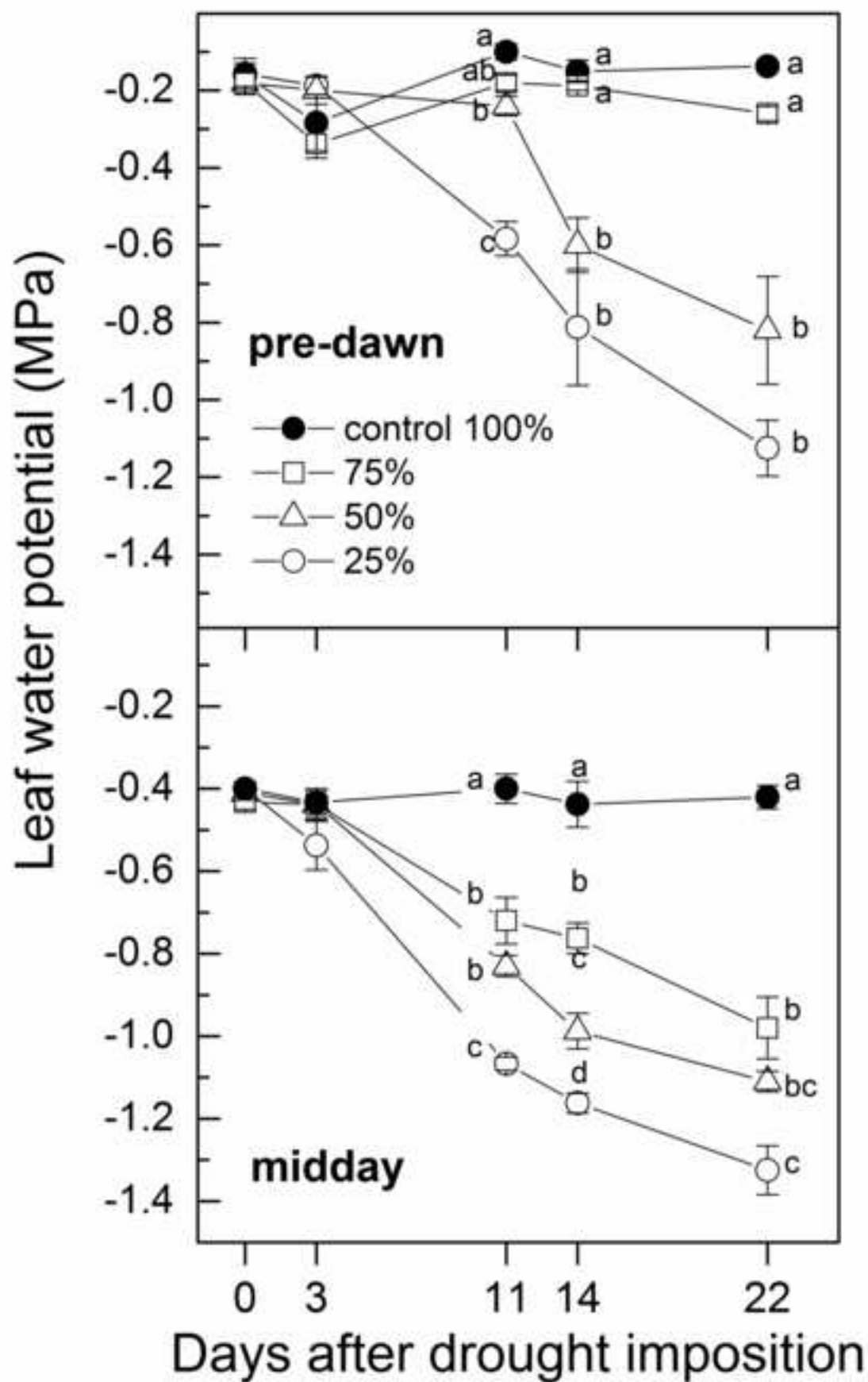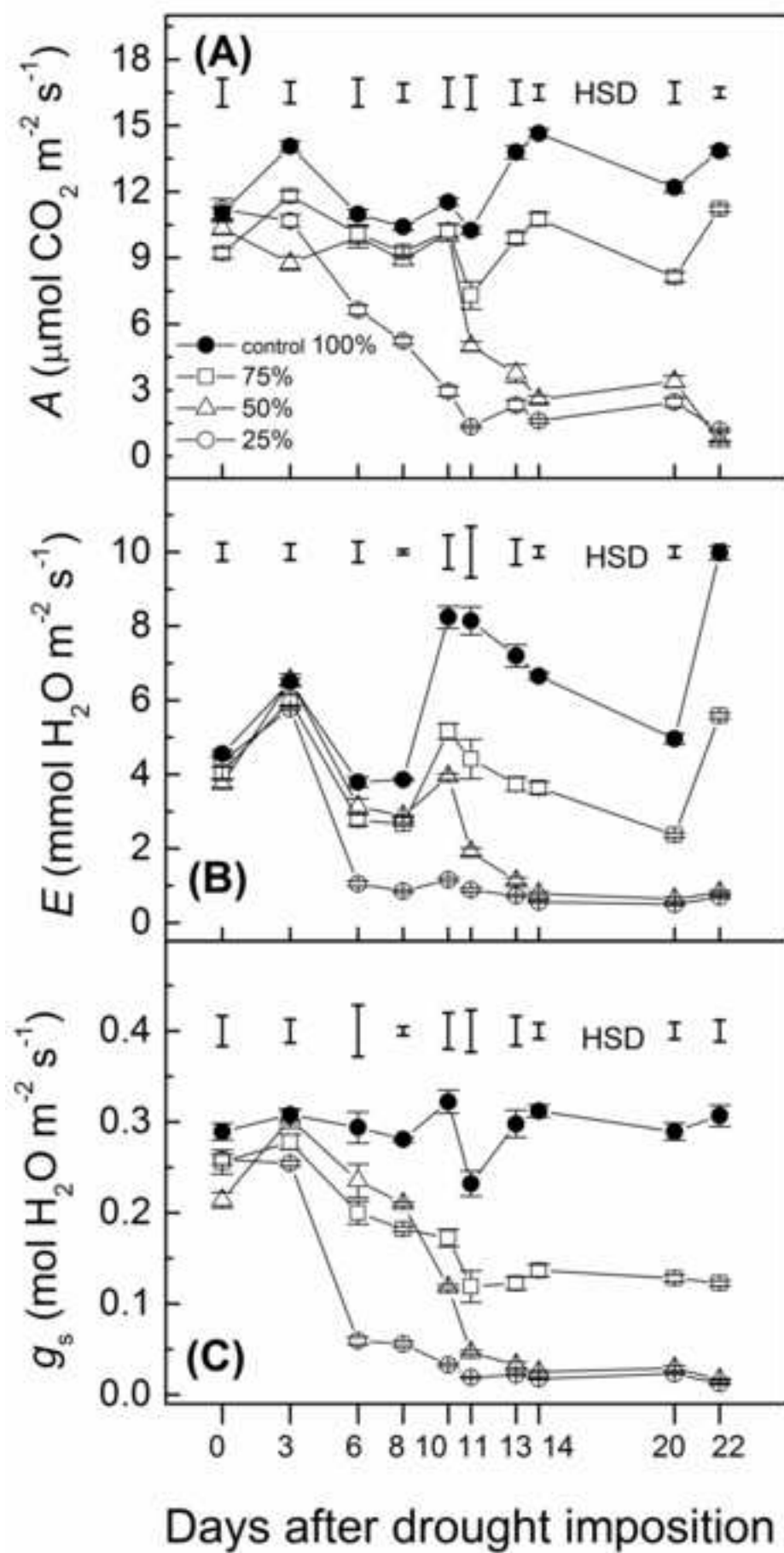
Figure 5
Click here to download high resolution image
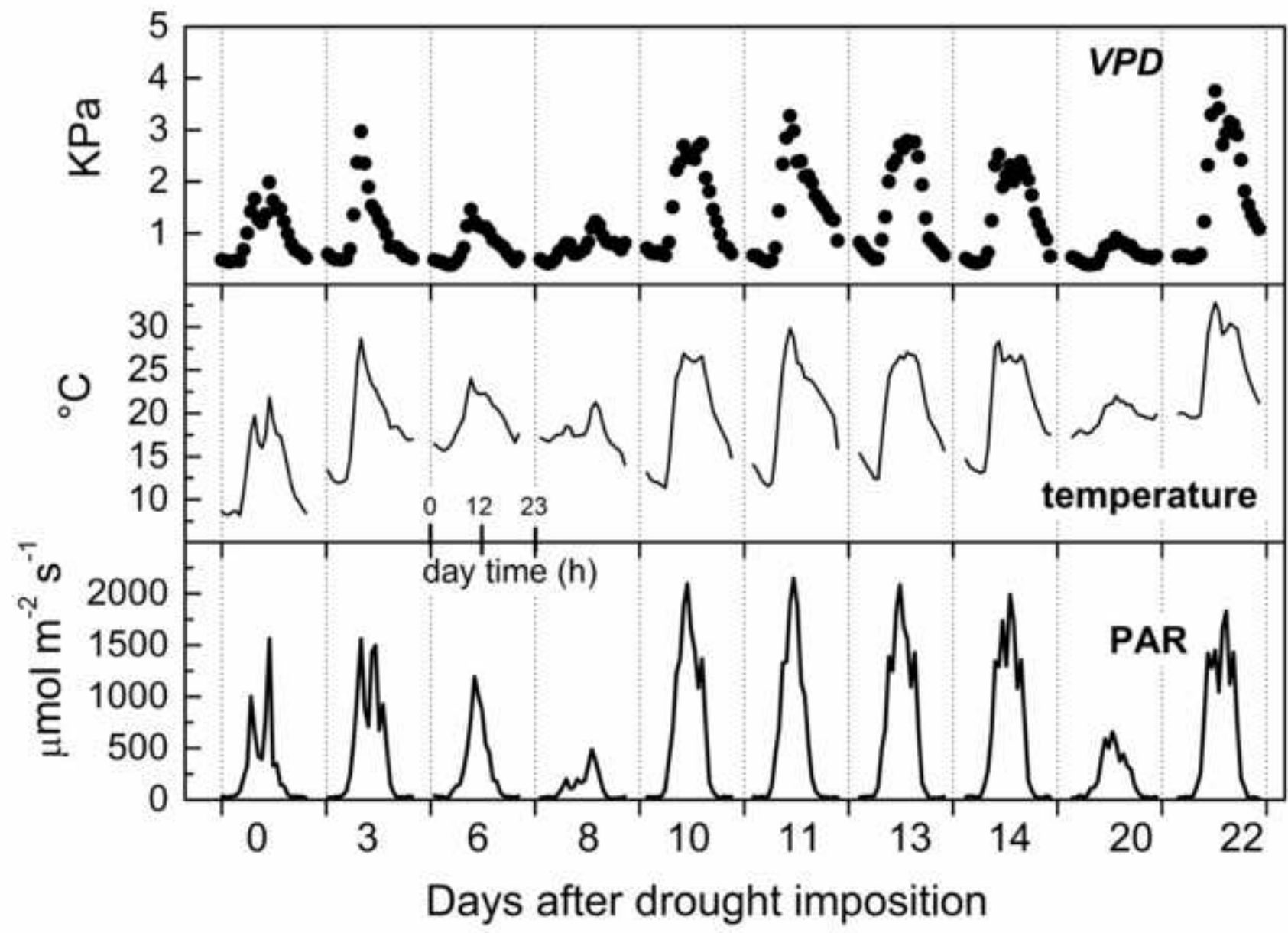
Figure 5

Figure 6
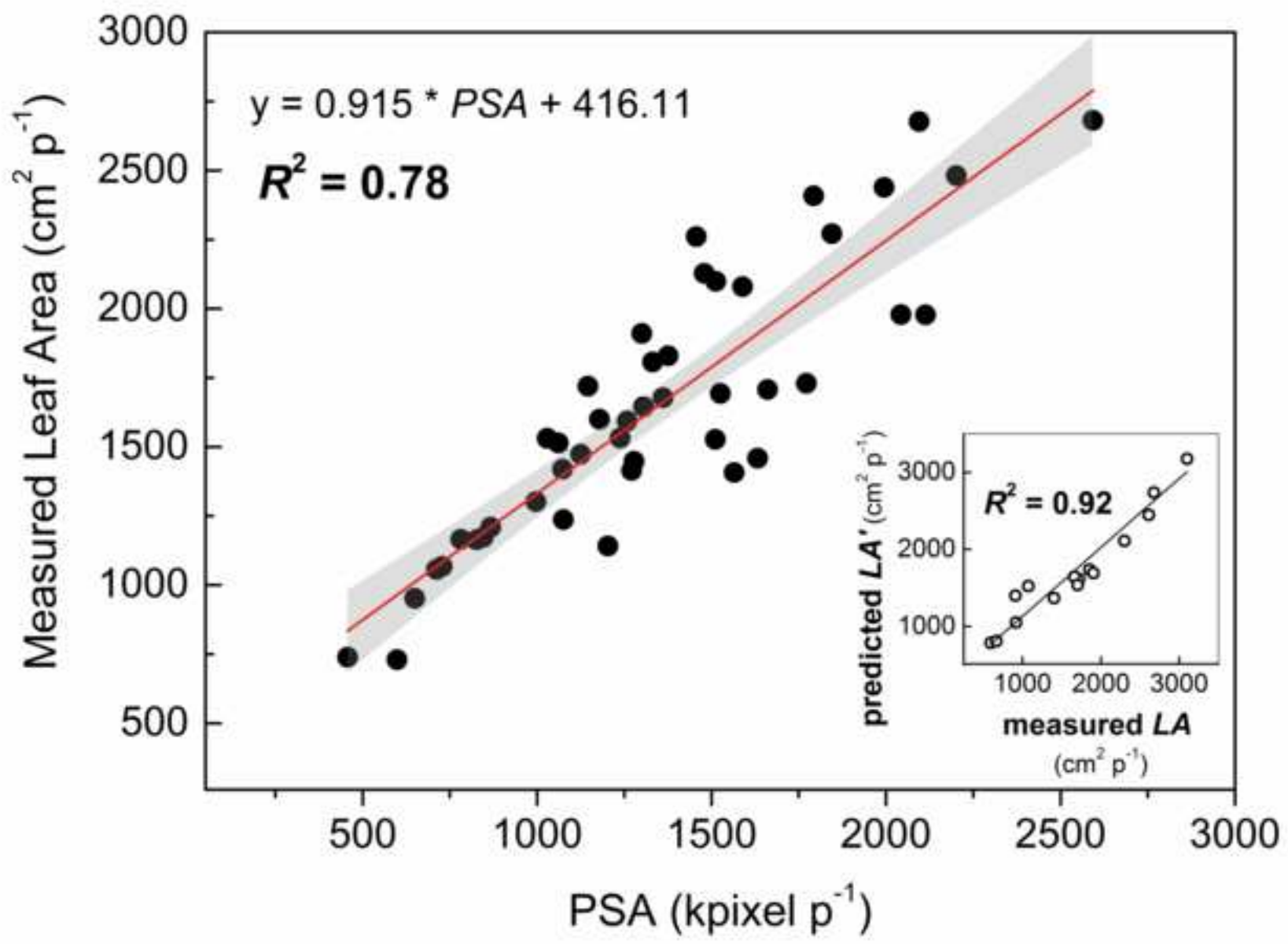**Click here to download high resolution image**
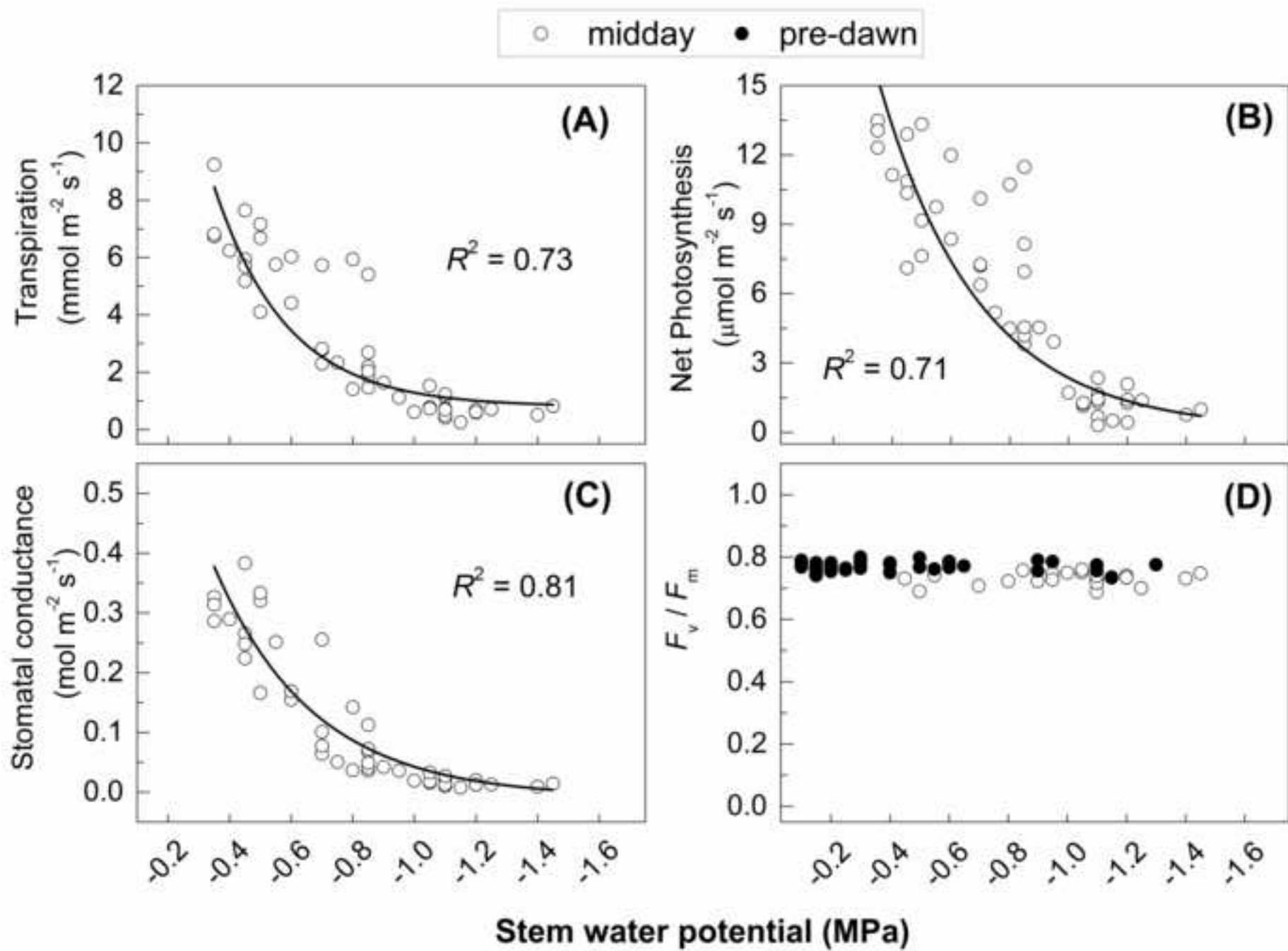
Figure 6

Figure 7

Figure 8
Click here to download high resolution image

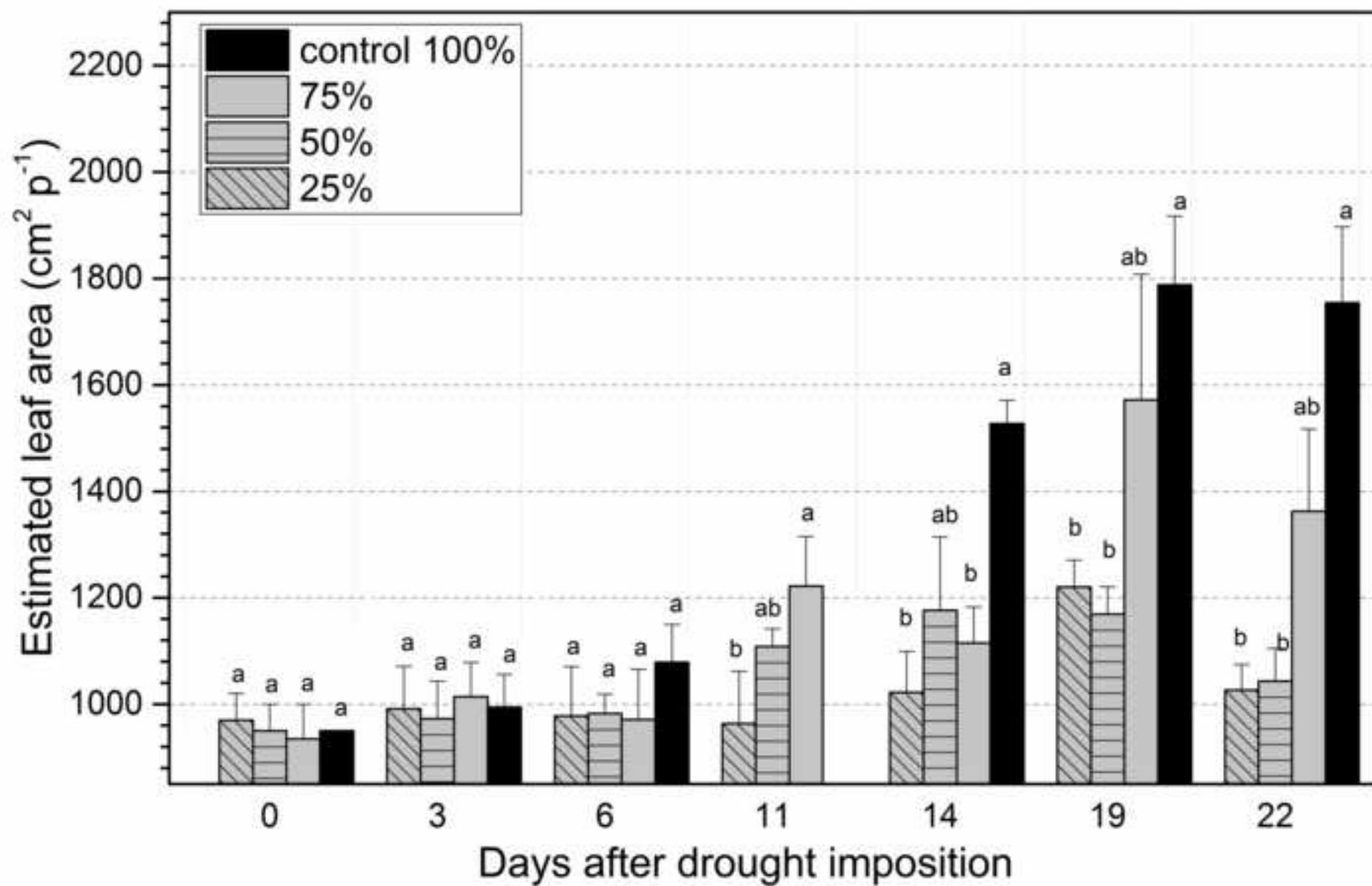**Figure 9**
Click here to download high resolution image

$R^2 = 0.86$

Figure 10
Click here to download high resolution image

Figure 10

Figure 11